Cathode Properties of Sodium Manganese Hexacyanoferrate in Aqueous Electrolyte

Nakamoto, Kosuke
Interdisciplinary Graduate School of Engineering Sciences, Kyushu University

Sakamoto, Ryo
Interdisciplinary Graduate School of Engineering Sciences, Kyushu University

Kitajou, Ayuko
Institute for Materials Chemistry and Engineering, Kyushu University

Ito, Masato
Institute for Materials Chemistry and Engineering, Kyushu University

他

https://doi.org/10.5109/1808305

Cathode Properties of Sodium Manganese Hexacyanoferrate in Aqueous Electrolyte

Kosuke Nakamoto[1], Ryo Sakamoto[1], Ayuko Kitajou[2],
Masato Ito[2], Shigeto Okada[2,*]

[1] Interdisciplinary Graduate School of Engineering Sciences, Kyushu University,
6-1 Kasuga-koen, Kasuga, Fukuoka 816-8580, Japan
[2] Institute for Materials Chemistry and Engineering, Kyushu University,
6-1 Kasuga-Koen, Kasuga, Fukuoka 816-8580, Japan

*Corresponding author, E-mail: s-okada@cm.kyushu-u.ac.jp

Aqueous sodium-ion batteries have been proposed as an attractive alternative to large-scale energy storage in terms of safety and economic efficiency. We experimentally confirmed that the potential width of the practical electrochemical window of a highly concentrated aqueous $NaClO_4$ electrolyte had 2.8 V by using the method of cyclic voltammetry. This positive effect allowed the $Na_2MnFe(CN)_6$ cathode to operate reversibly at unusually higher potentials in highly concentrated aqueous electrolyte without any side reactions such as undesirable oxidation of water.

1. Introduction

Safe and low-cost large-scale energy storage has become more and more important with the increasing demand for efficient utilization of sustainable energy resources, including solar and wind power. Lithium-ion batteries (LIBs) have been applied not only to small but also to medium-sized electricity storage systems, but the development of large-scale storage systems has been delayed in view of the safety and economic issues. Since the high energy density of LIBs depends on flammable organic electrolytes, rigorous exclusion of air and moisture is required to ensure adequate security and to prevent fatal accidents. In addition, there are numerous factors contributing to the high cost. In particular, LIBs run the risk of a supply shortage of the Li and minor metals required as cathode active materials. It is well known that the simple replacement of Li with Na in the electrolyte and electrodes does not lead to an analogous sodium-ion battery (SIB), because the volume of the Na ion is twice that of Li. Nevertheless, we believe that the exploration of Na-based electrode active materials, which may operate in aqueous electrolytes under the same principle as the intercalation mechanism at ambient temperature, could offer an effective solution to address these issues. The fundamental challenge for the development of such an aqueous sodium-ion battery (ASIB) is to overcome the narrow operating potential range for aqueous electrolytes to achieve higher energy density. In this respect, it is notable that the water decomposition is suppressed in highly concentrated aqueous lithium-ion batteries (ALIBs)[1-4]. In the previous report about ALIBs, it was observed that the almost of water molecules hydrated to highly concentrated Li^+ by NMR, Raman spectrometry and the method of molecular dynamics simulation. It was interpreted that the hydration reduces the activity of water and suppresses the water decomposition[1]. Quite recently, even in Na system, it was reported that a highly concentrated aqueous solution containing $NaClO_4$ allows the high voltage operation of cathode materials[5,6].

In this paper, in order to confirm the positive effect of the highly concentrated aqueous electrolyte, we measure the electrochemical window of the diluted and concentrated $NaClO_4$ aqueous electrolytes, respectively. In addition, the application of a highly concentrated aqueous $NaClO_4$ electrolyte to ASIB with a NASICON-type $NaTi_2(PO_4)_3$ anode[7,8] and Prussian blue-type $Na_2MnFe(CN)_6$ cathode[6,9-13] is also shown.

2. Experimental

$Na_2MnFe(CN)_6$ (NMHCF) was prepared by the conventional co-precipitating method[14,15] and characterized by X-ray powder diffraction (XRD, 50 kV and 300 mA, Cu-Kα, RINT2100HLR/PC, Rigaku Corp.), scanning electron microscopy (SEM, JSM-6340F, JEOL Ltd.), inductively coupled plasma-atomic emission spectroscopy (ICP-AES, Optima 8300, PerkinElmer Co., Ltd.), atomic adsorption spectrophotometry (AAS,
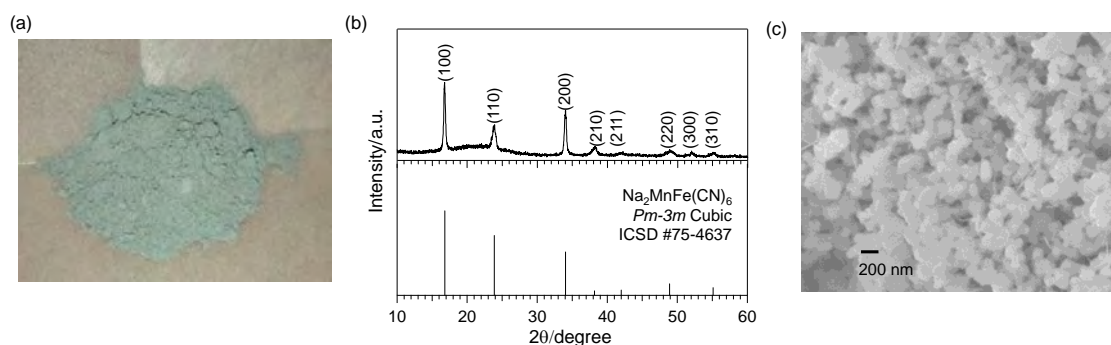
Fig. 1: (a) Photo image, (b) XRD pattern and (c) SEM image of as-prepared NMHCF powder.
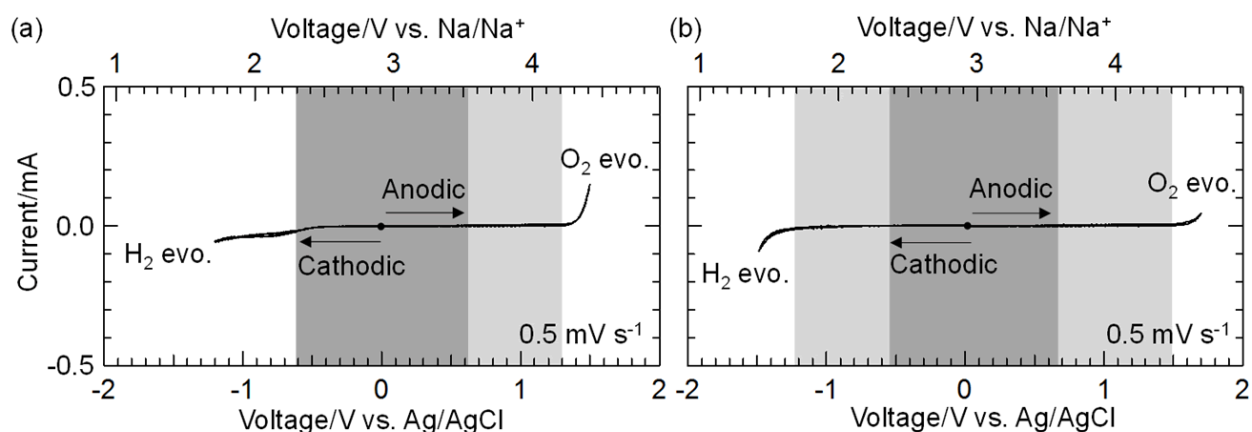

Fig. 2: Cyclic voltammograms of (a) 1 m NaClO$_4$ aq. and (b) 17 m NaClO$_4$ aq., respectively.

Z-5310, Hitachi High-Tech Science Corp.), and thermo-gravimetric analysis (TGA, Thermo Plus TG8110, Rigaku Corp.). NaTi$_2$(PO$_4$)$_3$ (NTP) was synthesized by the previously reported solid-state method.[8] NMHCF was mixed with acetylene black (AB) in a ratio of 70:25 (w/w) with a mortar and pestle. NTP was mixed with AB in a ratio of 70:25 (w/w) in a ball mill and the resulting mixture was annealed at 800 ℃ for 1 h under Ar+H$_2$ atmosphere.[7] These carbon composites were mixed with a polytetrafluoroethylene (PTFE) binder in a ratio of 95:5 (w/w) and molded into separate discs to use as cathode and anode, respectively (ca. 20 and 30 mg cm^{-2} for each and 200 μm thick). Titanium mesh was used as a current collector, a silver-silver chloride electrode/saturated KCl (Ag-AgCl) was used as a reference electrode, and an NTP disc was used as a counter electrode. Cyclic voltammetry (CV) and a galvanostatic charge/discharge cycle test were carried out with a three-electrode electrochemical cell using aqueous NaClO$_4$ solutions of varying concentrations as an electrolyte. The CV was performed with a Versastat 3 (AMETEK Inc.). Galvanostatic charge/discharge tests were carried out with a cycler (Nagano & Co., Ltd.) at various constant current densities. In the following context, "m" represents a molality unit (molality [m] = mole of solute / weight of solvent [mol kg^{-1}]) in

distinction from a molarity unit (molarity [M] = mole of solute / volume of solution [mol L^{-1}]).

3. Results and Discussion

XRD for prepared moss-green NMHCF powder (Fig. 1 (a)) showed cubic with a *Pm*-3m diffraction pattern, which was identified as Na$_2$MnFe(CN)$_6$ (ICSD # 75-4637). No other phases were detected, as illustrated in Fig. 1 (b). The morphology of ca. 200 nm-sized round particles observed by SEM (Fig. 1 (c)) was similar to that reported in the literature.[14] Elemental analyses for Mn and Fe by ICP-AES, and for Na by AAS, together with the measurement of water content by TG, revealed that the molecular formula was Na$_{1.24}$Mn[Fe(CN)$_6$]$_{0.81}$·1.28H$_2$O. Accordingly, its theoretical capacity was estimated as 120 mAh g^{-1}.

Figure 2 (a) and (b) shows the CV profiles of the titanium mesh current collector in 1 m and 17 m NaClO$_4$ aqueous electrolytes, respectively. The dark gray-colored areas in Fig. 2 (a) and (b) indicate the theoretical electrochemical window of water at each pH value of as-prepared aqueous electrolytes. On the other hand, the light gray-colored areas in Fig. 2 represent the practical electrochemical window of each electrolyte. As shown in Fig. 2 (a) and (b), the potential widths of the practical electrochemical windows of diluted 1 m and

concentrated 17 m $NaClO_4$ aq. were estimated to be approximately 1.9 V and 2.8 V, respectively.

Figure 3 (a) and (b) shows the concentration dependence of the electrolyte on the cyclability and charge/discharge profile of NMHCF for each electrolyte, respectively. The NMHCF cathode in the more highly concentrated electrolytes showed better cyclability and smaller irreversible capacity. On the other hand, the higher-voltage plateau of cycled profiles accompanying Mn^{2+}/Mn^{3+} redox vanished, especially in the diluted electrolyte, as shown in Fig. 3 (b). The cathode could deteriorate and its impedance could increase because of the incomplete suppression of water decomposition in diluted electrolyte. This means that the highly concentrated electrolyte would be expected to contribute to the stable operation of the aqueous Na-ion battery at the higher voltage by extending the practical stability window.

Figure 3 (c) and (d) shows the rate capabilities and charge/discharge profiles of NMHCF at various C rates in 17 m $NaClO_4$ aqueous electrolytes, respectively. Here,

the C rate is defined as the current required to discharge the theoretical capacity (120 mAh/g) in 1 h. For example, 2C is the current required to discharge the nominal capacity in 30 min and 0.5C is the current required to discharge the nominal capacity in 2 h, respectively. As shown in Fig. 3 (d), from 0.83C to 8.3C, there are few differences in the charge/discharge profiles of the 1st, 10th and 100th cycles. However, when the lower rate was used, the higher plateau of the profiles of 100th cycle disappeared. Even in the highly concentrated $NaClO_4$ electrolyte, the small charge/discharge overpotential at the lower rate could not completely suppress the water decomposition, and the cathode deteriorated, which was also observed in several previous reports.[1,16,17] On the other hand, in the case of higher rates, the profiles of the 100th cycle did not exhibit higher plateaus, while lower plateaus almost remained. In particular, the higher plateau on the 1st profile vanished at 42C. This could be well explained by the fact that the Warburg diffusion resistance of the Mn^{2+}/Mn^{3+} state is larger than that of Fe^{2+}/Fe^{3+} in NMHCF, as previously reported.[6]
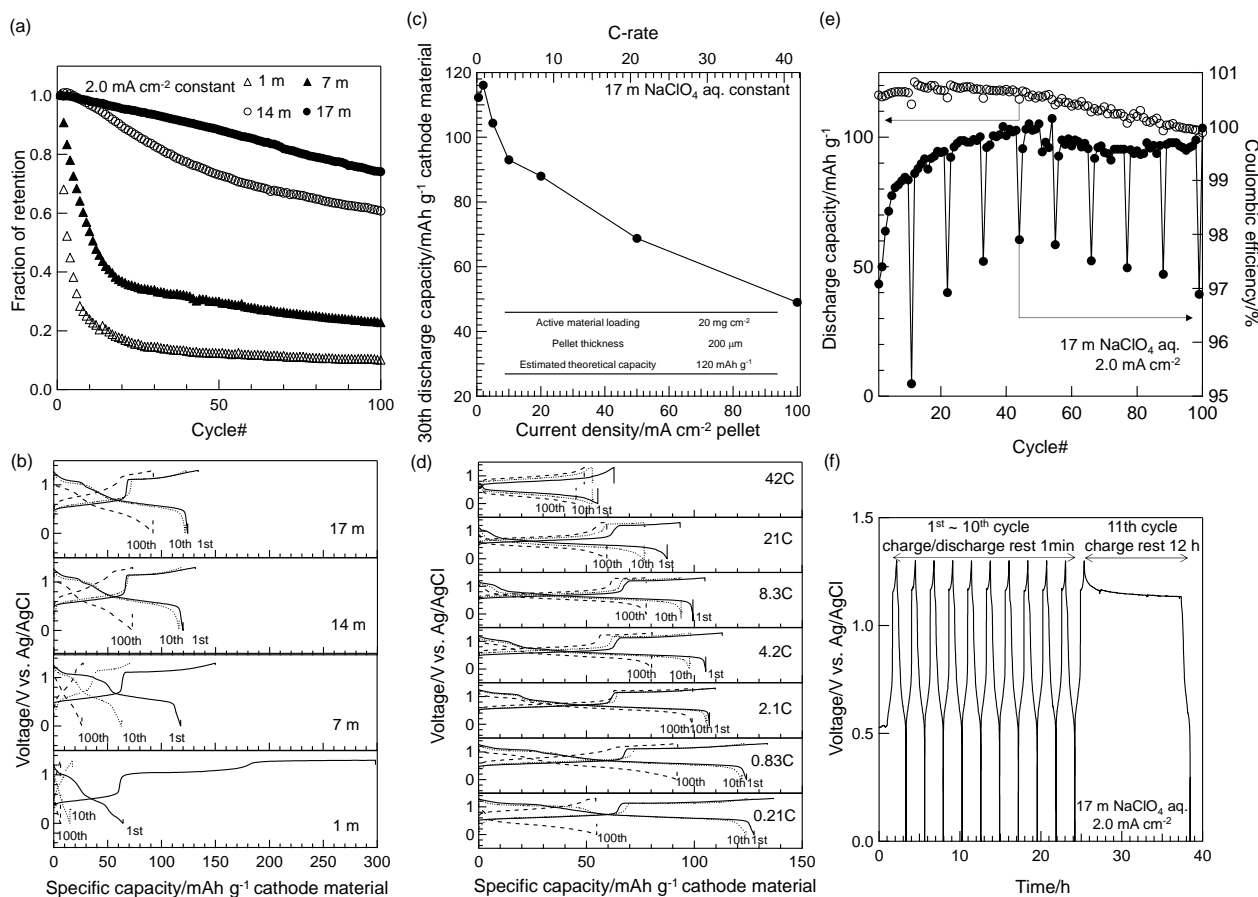

Fig. 3: (a) Cyclabilities and (b) charge/discharge profiles of NMHCF at a rate of 2.0 mA cm^{-2} in various concentrated $NaClO_4$ aqueous electrolytes. (c) Rate capabilities at 30th cycle and (d) charge/discharge profiles at 1st, 10th and 100th cycle of NMHCF in 17 m $NaClO_4$ aqueous electrolyte at various C rates. (e) Cycle performances and coulombic efficiency of NMHCF//NTP full cell after every 10 cycles resting 12 hours at fully charged to 1.3 V, and (f) the voltage decay of NMHCF//NTP full cell with 17 m $NaClO_4$ aqueous electrolyte at rest after fully charging to 1.3 V in the 11th cycle.

To evaluate the stability of the aqueous cell with the 17 m concentrated $NaClO_4$ electrolyte, the cycle performances and coulomb efficiency of the NMHCF// NTP cell were measured. In this cycle test, 12 h long rest periods were inserted after charging up to 1.3 V every 10 cycles. As shown in Fig. 3 (e), the average coulombic efficiency of the cycles with 1 min rest was approximately 99%, while that of the cycles with 12 h rest after charging was approximately 97%. Although the open circuit voltage decay of the NMHCF//NTP cell was observed during 12 h rest period, there were few differences between the discharge profiles after 1 min rest and those after 12 h rest, as shown in Fig. 3 (f). These results indicate that the recoverable capacity even after 12 h rest was not inferior to that after 1 min rest, and side reactions or self-discharge of fully charged NMHCF//NTP with 17 m concentrated $NaClO_4$ electrolyte were not observed.

4. Conclusion

We revealed that 1 m and 17 m $NaClO_4$ aq. have 1.9 and 2.8 V of practical stability windows, respectively. By virtue of its 2.8 V extended practical stability window, the NMHCF cathode with 17 m $NaClO_4$ aq. could work reversibly in comparison with serious degradation in 1 m. Higher concentrations of aqueous electrolyte supported more stable operation of NMHCF. The much higher rate of 42C allowed Fe^{2+}/Fe^{3+} redox of NMHCF even with electrodes 200 μm-thicker than those of LIB. Even after a 12 h rest of NMHCF charged up to 1.3 V, a high coulomb efficiency of approximately 97% was exhibited. Therefore, we propose that the ASIB with an NMHCF cathode and 17 m highly concentrated electrolyte would be appropriate for large-scale energy storage.

References

1) L. Suo, O. Borodin, T. Gao, M. Olguin, J. Ho, X. Fan, C. Luo, C. Wang, K. Xu, *Science*, **350**, 938 (2015).

2) L. Suo, O. Borodin, W. Sun, X. Fan, C. Yang, F. Wang, T. Gao, Z. Ma, M. Schroeder, A. von Cresce, S. M. Russell, M. Armand, A. Angell, K. Xu, C. Wang, *Angew. Chem. Int. Ed.*, **55**, 7136 (2016).

3) C. Wessells, R. Ruffo, R. A. Huggins, Y. Cui, *Electrochem. Solid-State Lett.*, **13**, A59 (2010).

4) K. Miyazaki, T. Shimada, S. Ito, Y. Yokoyama, T. Fukutsuka, T. Abe, *Chem. Commun.*, **52**, 4979 (2016).

5) P. R. Kumar, Y. H. Jung, B. Moorthy, D. K. Kim, *J.Electrochem. Soc.*, **163**, A1484 (2016).

6) M. Pasta, R. Y. Wang, R. Ruffo, R. Qiao, H.-W. Lee, B. Shyam, M. Guo, Y. Wang, L. A. Wray, W. Yang, M. F. Toney, Y. Cui, *J. Mater. Chem. A*, **4**, 4211 (2016).

7) S. -I. Park, I. D. Gocheva, S. Okada, J. Yamaki, *J.Electrochem. Soc.*, **158**, A1067 (2011).

8) W. Wu, J. Yan, A. Wise, A. Rutt, J. F. Whitacre, *J.Electrochem. Soc.*, **161**, A561 (2014).

9) C. D. Wessells, S. V. Peddada, R. A. Huggins, Y. Cui, *Nano Lett.*, **11**, 5421 (2011).

10) X. Wu, Y. Cao, X. Ai, J. Qian, H. Yang, *Electrochem. Commun.*, **31**, 145 (2013).

11) X. Wu, M. Sun, Y. Shen, J. Qian, Y. Cao, X. Ai, H. Yang, *ChemSusChem.*, **7**, 407 (2014).

12) X. Wu, M. Sun, S. Guo, J. Qian, Y. Liu, Y. Cao, X. Ai, H. Yang, *ChemNanoMat*, **1**, 188 (2015).

13) X. Wu, Y. Luo, M. Sun, J. Qian, Y. Cao, X. Ai, H. Yang, *Nano Energy*, **13**, 117 (2015).

14) J. Song, L. Wang, Y. Lu, J. Liu, B. Guo, P. Xiao, J. J. Lee, X. Q. Yang, G. Henkelman, J. B. Goodenough, *J. Am. Chem. Soc.*, **137**, 2658 (2015).

15) L. Wang, Y. Lu, J. Liu, M. Xu, J. Cheng, D. Zhang, J. B. Goodenough, *Angew. Chem. Int. Ed.*, **52**, 1964 (2013).

16) J. -Y. Luo, W. -J. Cui, P. He, Y. -Y. Xia, *Nat. Chem.*, **2**, 760 (2010).

17) Y. Yamada, K. Usui, K. Sodeyama, S. Ko, Y. Tateyama, A.Yamada, *Nat. Energy*, **2**, 16129 (2016).